Journal of Petroleum Research and Studies

Open Access
Vol. 14, No. 2, June 2024, pp. 88-100

P- ISSN: 2220-5381
E- ISSN: 2710-1096

DOI: http://doi.org/10.52716/jprs.v14i2.866

Localized Corrosion Behavior of Carbon Steel as a Function of Surface Temperature and Water Condensation Rate at the Top of Oil and Gas Pipelines

Khalid A. Mohammed[1*], Hazim S. Hamad[2]

[1]Oil and gas department, College of Engineering, University of Thi-Qar, Iraq

[2]Midland Refineries Company (MRC), Ministry of Oil, Iraq

[*]Corresponding Author E-mail: HazimSaab7@gmail.com

Received 24/12/2023, Revised 04/02/2024, Accepted 07/02/2024, Published 12/06/2024

Abstract

Pitting corrosion in carbon steel can be complex and largely unpredictable, making it challenging to inhibit the propagation of pits once they have formed. The CO2 corrosion mechanism is subject to various influencing factors, including temperature, pH solution, and the duration of exposure to corrosive media. Additionally, the characteristics and structure of the protective films formed play a role in determining the likelihood of pit initiation and propagation on carbon steel surfaces.

This research explores the correlation between the pitting corrosion characteristics of carbon steel and varying surface temperatures and water condensation rates in CO2-saturated environments, specifically in the top-of-line scenario. The effect of the water condensation rate (WCR) on the TLC rate was investigated at surface temperatures of 15°C, and 40°C.

At a relatively low surface temperature of 15°C, Fig. **(6**results demonstrate that increasing the WCR above 0.712 ml/m^2·s.

Pitting corrosion was studied under different conditions using the surface profilometry technique. Understanding the kinetics of $FeCO_3$ film formation, including its presence and absence, is essential in assessing the potential for localized corrosion.

During a 7-day exposure period, under specific conditions of water condensation rate and steel temperature, a partially protective corrosion film developed. Nevertheless, localized corrosion was distinctly evident on the steel surface. Over time, pits appeared to be deepening, particularly at higher steel temperatures and the maximum depth was 50 μm at 50℃.

Keywords: Top of line corrosion; Surface temperature; Gas temperature; Condensation rate; Localized corrosion.

Journal of Petroleum Research and Studies

Open Access
Vol. 14, No. 2, June 2024, pp. 88-100

P- ISSN: 2220-5381
E- ISSN: 2710-1096

سلوك التآكل النقري للفولاذ الكربوني بدلالة درجة حرارة السطح ومعدل تكثف الماء في الجزء العلوي من أنابيب النفط والغاز

الخلاصة:

يعد التأكل النقري (pitting corrosion) في الانابيب النفطية المصنوعة من الفولاذ الكربوني معقدا لايمكن تنبؤه الى حد كبير. مما يشكل تحديا كبيرا لمكافحة ومعالجة نمو التنقرات بمجرد تشكلها.

تأكل ثاني أكسيد الكربون في انابيب الفولاذ يتأثر بعدة عوامل منها درجة الحرارة ودرجة الحامضية (PH) في الموقع وزمن التعرض للبيئة المسببة للتآكل ونوع المحلول الكيميائي (مثل نسبة تركيز ايون الكلوريد).

بالإضافة إلى ذلك مواصفات وبنية الطبقة المشتكلة الحامية التي تلعب دوراً رئيسيا في أحتمال نشوء التنقرات المتكونة وانتشارها على الأسطح المصنوعة من الصلب الكربوني.

يستكشف هذا البحث العلاقة بين خصائص التآكل النقري في الكاربون الصلب ودرجة حرارة سطح المعدن ونسبة الماء المكثف على السطح العلوي في وسط مشبع بالكاربون بالأخص منطقة السطح العلوي للانبوب وتحديد أفضل سيناريو.

تمت دراسة تآكل التنقر تحت ظروف مختلفة باستخدام تقنية مقياس السطح مع فهم آلية حركة تكوين الطبقة الـ $FeCO_3$، بما في ذلك تقييم احتمالية التآكل الموضعي في حال وجود او عدم تكون طبقة حامية خلال فترة تعرض مدتها 7 أيام، في ظل ظروف محددة لمعدل تكثف الماء ودرجة حرارة الفولاذ.

تم تطويرطبقة واقية من التآكل جزئيًا. ومع ذلك، التآكل النقري كان ظاهراً بشكل واضح على سطح الفولاذ. مع مرور الوقت، بدا أن الحفر تتعمق، خاصة في درجات حرارة الصلب العالية.

1. Introduction:

Top -of –the- line- corrosion (TLC) is one of many types of corrosion and can be considered as one of the most recent to be discovered, as it was first recognized in the 1990s [1].

Within the oil and gas sector, the crude oil transportation in in carbon steel pipelines is a vital step. Typically, most oil transporting pipelines are made from carbon steel which can corrode easily under flowing conditions; this will lead to a loss of pipeline safety and integrity and most importantly loss of oil production.

The TLC phenomenon happens when there is substantial heat exchange between the saturated vapour flowing through the pipeline and the environment surrounding the pipe. This leads to condense the water vapor, forming droplets or a thin film of liquid at the top of the pipe and on the cold walls of the pipeline. The condensed water may include dissolved corrosive species and gases like carbon dioxide (CO_2) and hydrogen sulfide (H_2S).

In CO_2 and H_2S environments, the occurrence of the localized corrosion of carbon steel is commonly present [2-8]. The mechanism of the localized corrosion at the top of line scenario and the questions of how the local oil field environment such as temperature and condensation rates could be influencing the pitting corrosion kinetics, pit initiation and pit propagation of top

Open Access
Vol. 14, No. 2, June 2024, pp. 88-100
P- ISSN: 2220-5381
E- ISSN: 2710-1096

of carbon steel pipelines exposed to oilfield corrosion environments are still not fully understood.

The available literature regarding the pitting corrosion mechanism of carbon steel materials in environments containing CO_2 and H_2S has outlined the following stages [2]:

1) Formation of $FeCO_3$ and FeS protective layers due to the corrosion processes of metal.
2) Remove of protective layers and localized breakdown occurs.
3) Anodic dissolution of materials at the sites where the breakdown of protective corrosion products layers takes place, while the respect to the rest of the film covered surface becomes sites of cathodic reactions.
4) Due to sufficient anodic dissolution rate, pit growth rate at localized anodic site will continue.

The effect of temperature on general and pitting corrosion rate in environment containing CO2 can be associated with the pH solution level. At low solution pH, the corrosion rate of carbon steel increases steadily with temperature. At these conditions the protective layer of iron carbonate film do not form [9, 10]. When the conditions change, at high level of pH, increasing temperature accelerates the kinetics of precipitation and protective scale formation, suppressing corrosion rates significantly. Also, the literature has shown that the precipitation of iron carbonate film on the pipeline surfaces does not necessarily result in the formation of a protective film.

At higher temperatures, the iron carbonate film texture becomes more crystalline and generally more protective. On the other hand, at temperatures less than 60°C, the corrosion scale has a smudge-like texture and is can be removed easily by the flow of fluid [10]. The previous studies have illustrated that, the corrosion rates are lowest at the lowest condensation rate because the expected renewal rate of condensed droplets is slower. The attainment of iron carbonate saturation is more achievable when liquid droplets remain attached to the pipe surface for a longer time [11]. The lack of ability to predict localized corrosion and to detect it by using conventional corrosion monitoring methods makes a difficult situation even worse. The present study explores the time-dependent progression of pitting corrosion on carbon steel in varying surface temperature and water condensation rates within CO_2-saturated environments, specifically in a scenario resembling the top of a pipeline. This allows to correlate the evolutions behaviour of pitting corrosion with surface temperature and condensation rate within CO_2-saturated environments, specifically in a scenario resembling the top of a pipeline.

Open Access
Vol. 14, No. 2, June 2024, pp. 88-100
P- ISSN: 2220-5381
E- ISSN: 2710-1096

The paper is organised as follows. **Section 2** describes the experiment methodology and the specification of the test samples. **Section 3** presents the experimental results which demonstrate the effect of temperature variations ate rate on pit growth. Finally, conclusions are drawn in **Section 4**.

2. Experimental Method

In this paper, a specialized CO2 corrosion setup was established to investigate the in-situ development of corrosion product layers and the localized breakdown of these products, potentially leading to pitting corrosion in carbon steel materials during a 168-hour testing period.

The test samples were made from X-65 grade carbon steel, which was in a normalized state, exhibiting a ferrite-pearlite microstructure. The Table (1) outlines the nominal composition of the X-65 steel.

Table (1): The typical chemical composition of the X-65 Carbon Steel

C	**Si**	**Mn**	**P**	**S**	**Cr**	**Mo**	**Ni**
0.12	0.18	0.127	0.008	0.005	0.11	0.25	0.25
Cu	**Sn**	**Al**	**P**	**Nb**	**Ti**	**V**	**Fe**
0.1	0.008	0.022	0.008	0.04	0.001	0.057	bal

2.1 Sample preparation

The preparation of samples for corrosion testing was standardized across tests conducted in CO_2-containing environments. The typical sample preparation procedure involved cutting the carbon steel sample to the desired dimensions of 10 mm x 10 mm x 5 mm, resulting in an exposed surface area of 1.00 cm^2. Before starting the experiment, the specimens were wet ground up to a grit size of 1200 using silicon carbide paper. Following that, the ground surfaces underwent degreasing with acetone, then, rinsing with distilled water, and drying with compressed air before being immersed in the solution.

2.2 Experimental procedure

The setup comprises a 2-liter glass cell capable of accommodating three test samples, as illustrated in Fig. (**1**).

Open Access
Vol. 14, No. 2, June 2024, pp. 88-100
P- ISSN: 2220-5381
E- ISSN: 2710-1096

Prior to each test, calibration of the pH probe and pH meter is performed, and the pH value was specified and maintained at specific value of 5.5 during the experiments. The test solution is then sparged with CO2 gas for at least 12 hours to de-aerate the solution to a level of less than 20ppb and achieve full saturation with CO2 gas. A small funnel was positioned directly beneath one of the samples to gather condensed water. This condensate was then directed into a sealed collection vessel to measure the rate of water condensation.

At the end of each test, the samples were cleaned with Clark's solution to eliminate all corrosion products before calculating the pitting corrosion rates. Additionally, certain samples were washed, allowed to air dry, and then meticulously stored in a de-aerated chamber to prevent oxidation of corrosion products before conducting surface analysis.

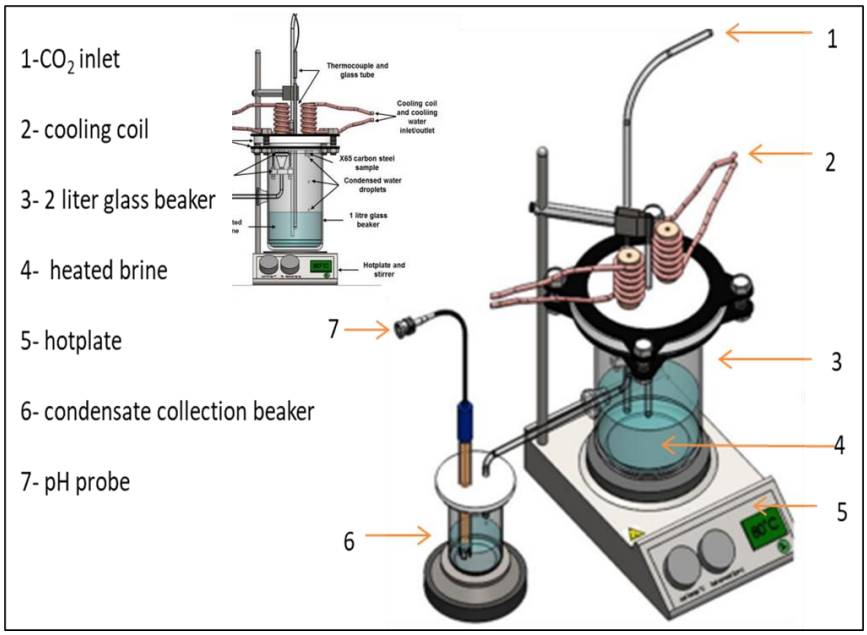

Fig. (1): Schematic of experimental setup

3. Results and Discussion

The study focused on investigation the behavior of the pitting corrosion of X-65 carbon steel within CO_2-saturated environments, specifically in a top-of-line scenario. This investigation involved varying surface temperatures and water condensation rates as key parameters.

Surface profilometry was carried out on each sample which was cleaned first by Clarke's solutions to eliminate any corrosion product residues that might hinder the accurate detection and quantification of pits. The analysis of pit depth adhered was based on the guidelines outlined in ASTM Standard [12], which recommends considering the average of the ten deepest

Open Access
Vol. 14, No. 2, June 2024, pp. 88-100
P- ISSN: 2220-5381
E- ISSN: 2710-1096

pits as well as the maximum pit depth for characterizing pit damage within the sample area.

3.1 Effect of Steel Surface Temperature on localized corrosion rate

In this study the influence of temperature variations on corrosion behaviour in a CO_2-saturated environment is explored by conducting a series of experiments test over a period of 168 hours at three different temperatures 30°C, 40°C and 50°C. The primary focus of these experiments was to gain insights into the corrosion kinetics and film formation as time progressed and to understand the role of temperature in these specific environments. A series of experiments were carried out for 168 hours under conditions conducive to the formation of a protective film of partial iron carbonate.

The surface temperature was maintained at 30°C, and the water condensation rate (WCR) was set at 0.326 ml/m^2. s, simulating conditions similar to those at the top of a wet gas transportation pipeline. During these experiments, the localized corrosion behaviour was determined, and a consistent and continuous pit growth was found. The maximum depths of the pits increased from approximately 7µm after 24 hours to approximately 25µm after 168 hours, as demonstrated in Fig. (**2**).

Furthermore, the findings revealed a direct correlation between pit depth and exposure time, suggesting that the presence of amorphous $FeCO_3$ had little to no impact on inhibiting pit propagation. Surprisingly, it is possible that the formation of the iron carbide (Fe_3C) layer might even enhance pitting corrosion in other localized anodic regions due to a potential galvanic reaction.

Fig. (**2**) illustrates the changes in relative pit depth (both maximum and average) over 168-hour duration at 30°C in a 3% wt. of NaCl solution. The error bars on the graph represent the standard deviation of the measurements of the 10 deepest pits.

The pit depths depicted in Fig. **(2** are measured relative to the corroded surface. Therefore, if the general corrosion rate rises while the pit growth unchanged and remains constant, the relative growth of pits may appear to decrease. Consequently, the observed increase could be attributed to galvanic reactions between iron carbide and the carbon steel surface, as proposed by Crolet et al. [13]. As evident from Fig. (**2**), the depth of localized attack measured after 168 hours of exposure is nearly 3.5 times greater than the one measured after 24 hours of testing. This suggests that the TLC (top of the line corrosion) may have considerably slowed down.

Open Access
Vol. 14, No. 2, June 2024, pp. 88-100
P- ISSN: 2220-5381
E- ISSN: 2710-1096

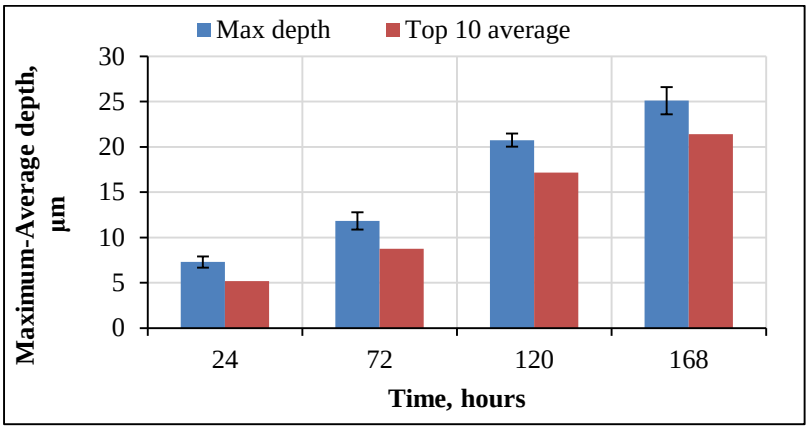

Fig. (2): Changes of maximum and average pit depth with time at a steel surface temperature of 30°C

Fig. (**3**) shows the pitting corrosion growth on carbon steel at 40°C which indicating that there is a consistent and linear growth rate of pits, starting from approximately 9 µm after 24 hours and progressing to 42 µm after 168 hours. Interestingly, although there is evidence of a protective iron carbonate layer formation, this specific corrosion product morphology does not seem to have the same effect on reducing the general corrosion rate as it does on inhibiting pit propagation. The continuous growth of pits could be attributed to the formation of the non-uniform of the iron carbonate film on the surface of the sample, resulting in a semi-protective nature of the corrosion product layer at this temperature.

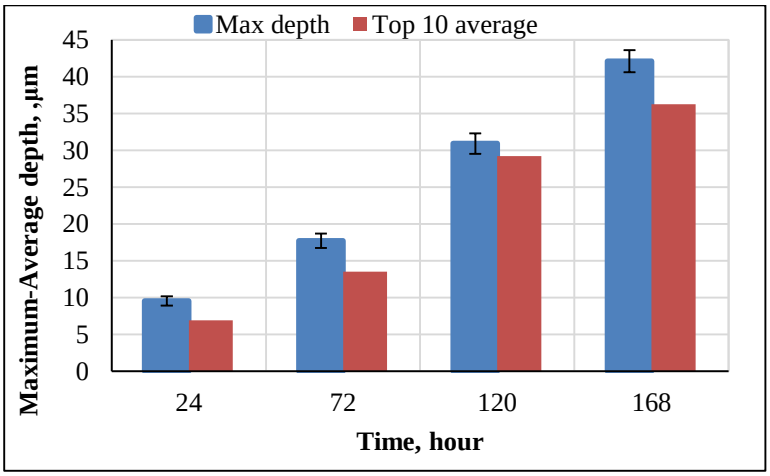

Fig. (3): Changes of maximum and average pit depth with time at a steel surface.

The behavior of the pitting corrosion of carbon steel at a temperature of 50°C is illustrated in Fig. (**4**). As pits were initiated, a consistent growth of pits was observed between 24 and 72 hours. During this time, the corrosion product layer primarily consisted of iron carbide (Fe_3C)

Open Access
Vol. 14, No. 2, June 2024, pp. 88-100
P- ISSN: 2220-5381
E- ISSN: 2710-1096

along with very small crystals of $FeCO_3$. After 72 hours, a slightly decreased pit growth rate was noticed.

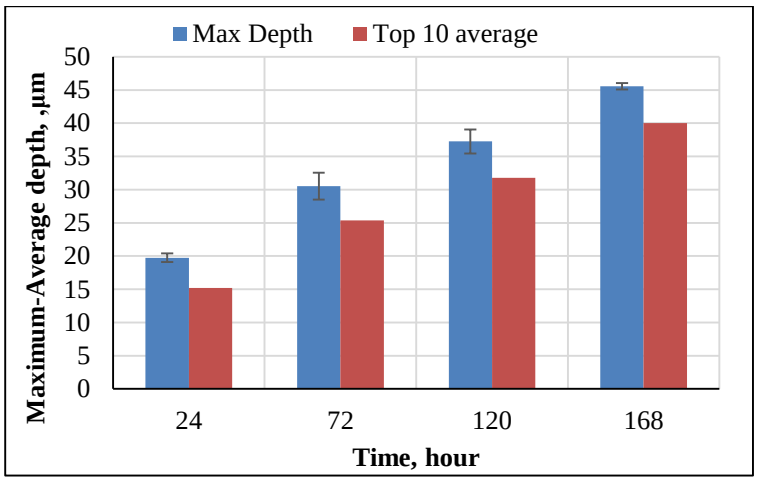

Fig. (4): Changes of maximum and average pit depth with time at a steel surface temperature of 50°C

Fig. (**5**), shows how the depth of the initiated micro pit is affected by the temperature variations and demonstrates clearly how the increases of the surface temperature increase the depth of propagation pit throughout the entire duration of the experiments.

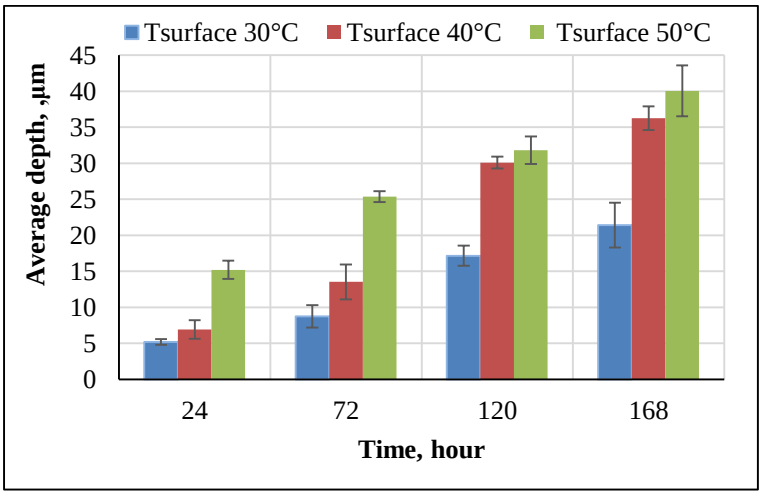

Fig. (5): Changes in relative average pit depth with time at three different surface temperatures: 30°C, 40°C, and 50°C

It is essential to consider the typical microstructure of X65 pipeline before initiating the corrosion process.

Typically, X65 pipeline steel consists of irregular ferrite and pearlitic grains. The microstructure of carbon steel includes layers of ferrite and cementite (Fe3C) forming the

Open Access
Vol. 14, No. 2, June 2024, pp. 88-100
P- ISSN: 2220-5381
E- ISSN: 2710-1096

pearlite phase, with the ferrite phase constituting 88 wt.% [1]. Research studies [5, 14-16] have indicated that during the corrosion reaction of steel in CO2-saturated environments, ferrite is preferentially dissolved from the steel surface. Consequently, the uncorroded cementite (Fe_3C) phase remains behind as a result of the anodic dissolution of ferrite and becomes the preferred sites for cathodic reduction reactions of H_2CO_3 and HCO_3^- [5, 17, 18]. This overall corrosion behavior, encompassing both general and pitting corrosion, is observed in carbon steel materials exposed to CO_2 environments.

The majority of chemical, electrochemical, and transport processes within the system, including H+ reduction, H_2CO_3 and HCO_3^-reduction, are known to accelerate with rising temperatures. This, in turn, leads to increased cathodic and anodic reactions [18, 19]. Consequently, any potential galvanic reactions occurring between iron carbide regions and exposed areas of localized pores, along with the associated corrosion kinetics, becomes more pronounced at elevated temperatures. As a result, the pit growth at surface temperature of 50°C is more significant compared to 40°C and 30°C. This observation aligns with the findings reported by Papavinasam and colleagues[2], where they observed an increase in pitting corrosion rates from 10 mpy at temperatures ≤ 25°C to 80 mpy at temperatures ≥ 50°C.

3.2 Effect of the Water Condensation Rate on localized corrosion rate

This study focuses on investigating the influence of the condensation rate on the TLC rate. The impact of the water condensation rate (WCR) on the TLC rate was examined at surface temperatures of 15°C, and 40°C.At a relatively low surface temperature of 15°C, Fig. **(6** demonstrates that increasing the WCR above 0.712 ml/m2·s does not lead to a significant change in the TLC rate. Despite more than doubling the WCR from 0.712 to 1.53 ml/m^2. s, there was no significant impact on the corrosion rate.

On the contrary, in Fig. (**6**), at a high surface temperature (Ts=40°C), the corrosion rate values demonstrated a substantial increase with both elevated gas temperature and higher WCR. The experimental findings revealed that at a surface temperature of 40°C, the CR increased notably from 0.55 to 1.27 mm/y as the WCR was raised from 0.32 to 0.712 ml/m2.s.

Consequently, for higher surface temperatures, an elevated WCR played a crucial role in boosting the CR. Based on the concise explanation above, it becomes evident that at low steel temperature, the degree of corrosion at the top of the line can be attributed to the steel temperature rather than the WCR. This correlation is due to the fact that the kinetics of any

Open Access
Vol. 14, No. 2, June 2024, pp. 88-100
P- ISSN: 2220-5381
E- ISSN: 2710-1096

chemical or electrochemical reaction slows down at low temperatures, including the processes of iron dissolution and FeCO3 precipitation. The low iron dissolution results in a low concentration of Fe2+ in the condensed liquid, leading to minimal super saturation and very little to no accumulation of corrosion products on the steel surface. Consequently, at low surface temperatures, the corrosion reactions is primarily influenced by the temperature at which it occur – specifically, the temperature of the steel, which can be entirely different from the gas temperature.

On the whole, Fig. (**6**) demonstrates that the lowest rate of the corrosion at the upper part of the pipe occurred when the condensation rate was at its lowest. This observation can be attributed to the influence of the water condensation rate on the formation of the corrosion product layer ($FeCO_3$). When the condensed water droplets remain attached to the steel surface for an extended period, it becomes easier to reach the saturation point of $FeCO_3$. Consequently, at higher condensation rates, where the renewal of condensed water droplets happens more rapidly, the supersaturation of condensed water with $FeCO_3$ diminishes, leading to higher steel corrosion rates. Conversely, at lower condensation rates, the slower renewal of condensed water droplets results in higher saturation levels of $FeCO_3$, leading to reduced steel corrosion rates.

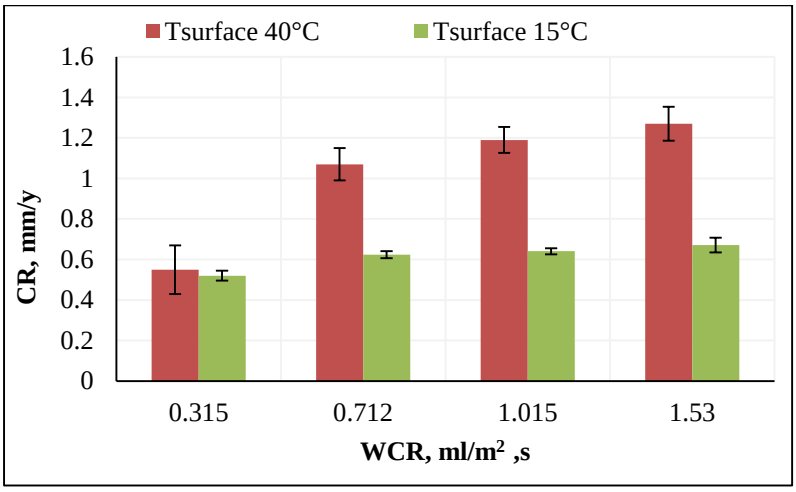

Fig. (6): The impact of the condensation rate on the corrosion rate after a 168-hour exposure

Open Access
Vol. 14, No. 2, June 2024, pp. 88-100
P- ISSN: 2220-5381
E- ISSN: 2710-1096

4. Conclusions

The study examined the correlation between the pitting corrosion characteristics of carbon steel when exposed to various surface temperatures and water condensation rates in CO2-saturated environments at the top-of-line scenario. By the analysis of the experimental result, the following conclusions can be summarized:

- The rate of initiation of pitting corrosion was found to increase with increasing temperature in carbon steel materials.
- The results indicated a clear link between pit depth and the duration of exposure, indicating that the presence of amorphous FeCO3 had minimal to no inhibitory effect on pit expansion.
- The initial micro pit depth exhibits a consistent rise as the temperature increases over the entire experimental duration.
- The top-of-the-line experienced its lowest average corrosion rate when the condensation rate was at its minimum. However, when the condensation rate increased, causing a more rapid renewal of condensed water droplets, the supersaturation of condensed water with FeCO3 decreased, resulting in higher rates of steel corrosion.

Acknowledgments: The authors would like to thank the Petroleum and gas department and Engineering College at the University of Thi-Qar and Midland Refineries Company (MRC) -Iraqi ministry of Oil for their scientific and technical support to establish this study.

Open Access
Vol. 14, No. 2, June 2024, pp. 88-100
P- ISSN: 2220-5381
E- ISSN: 2710-1096

References:

[1] M. Khalid Abdulhussain, "Experimental and theoretical investigation of top of the line corrosion in CO_2 gas and oil environments", PhD thesis, University of Leeds, 2018.

[2] S. Papavinasam, A. Doiron, and R. W. Revie, "Model to predict internal pitting corrosion of oil and gas pipelines", *Corrosion*, vol. 66, no. 3, p. 035006-035006-11, 2010. https://doi.org/10.5006/1.3360912.

[3] N. Anselmo, J. E. May, N. A. Mariano, P. A. P. Nascente, and S. E. Kuri, "Corrosion behavior of supermartensitic stainless steel in aerated and CO2-saturated synthetic seawater", *Materials Science and Engineering: A*, vol. 428, no. (1-2), pp. 73-79, 2006. https://doi.org/10.1016/j.msea.2006.04.107

[4] J. Soltis, "Passivity breakdown, pit initiation and propagation of pits in metallic materials–review", *Corrosion Science,* vol. 90, pp. 5-22, 2015. https://doi.org/10.1016/j.corsci.2014.10.006

[5] M. B. Kermani, and A. Morshed, "Carbon dioxide corrosion in oil and gas productiona compendium", *Corrosion,One Petro Journal*, vol. 59, no. 8, 2003.

[6] K. A. Mohammed, "Ethylated Amine Role in the Inhibition of Top of Line Corrosion in Marginally Sour Environments", *University of Thi-Qar Journal for Engineering Sciences*, vol. 12, no. 1, pp. 137-145, 2022.

[7] C. Liu, R. I. Revilla, X. Li, Z. Jiang, S. Yang, Z. Cui, D. Zhang, H. Terryn, and X. Li, "New insights into the mechanism of localised corrosion induced by TiN-containing inclusions in high strength low alloy steel", *Journal of Materials Science & Technology*, vol. 124, pp. 141-149, 2022. https://doi.org/10.1016/j.jmst.2021.12.075

[8] Z.Rinaldi, et al., "*Influence of localised corrosion on the cyclic response of reinforced concrete columns"*. Engineering Structures, 2022. **256**: p. 114037. https://doi.org/10.1016/j.jmst.2021.12.075

[9] S. Nešić, "Key issues related to modelling of internal corrosion of oil and gas pipelines–A review", *Corrosion science*, vol. 49, no. 12, pp. 4308-4338, 2007. https://doi.org/10.1016/j.corsci.2007.06.006

[10] C.De Waard, U. Lotz, and D. Milliams, "Predictive model for CO2 corrosion engineering in wet natural gas pipelines", *Corrosion*, vol. 47, no. 12, pp. 976-985, 1991. https://doi.org/10.5006/1.3585212

Open Access
Vol. 14, No. 2, June 2024, pp. 88-100
P- ISSN: 2220-5381
E- ISSN: 2710-1096

[11] M. Singer, S. Nesic, and Y. Gunaltun. "Top of the line corrosion in presence of acetic acid and carbon dioxide", *NACE CORROSION*, pp. NACE-04377, 2004.

[12] G46-94 , "Standard guide for examination and evaluation of pitting corrosion", *ASTM International*, 2005.

[13] M. Singer, D. Hinkson, Z. Zhang, H. Wang, and S. Nešić, "CO2 top-of-the-line corrosion in presence of acetic acid: a parametric study", *Corrosion*, vol. 69, no. 7, pp. 719-735, 2013. https://doi.org/10.5006/0737

[14] W. D. Callister, D. G. Rethwisch, A. Blicblau, K. Bruggeman, M. Cortie, J. Long, J. Hart, R. Marceauet, and R. Mitchell, "Materials science and engineering: an introduction", Vol. 7, pp. 665-715, New York: John wiley & sons, 2007.

[15] K. A. Mohammed, A. K. Okab, H. S. Hamad, M. Hashim, and R. K. Abdulhussain, "Drilling and casing pipes corrosion investi-gation in water based drilling mud of Iraqi oil fields environment", *Journal of Mechanical Engineering Research and Developments*, vol. 44, no. 8, pp. 232-240, 2021.

[16] J.Han, B. Brown, and S. Nešic, "Investigation of the galvanic mechanism for localized carbon dioxide corrosion propagation using the artificial pit technique", *Corrosion*, vol. 66, no. 9, p. 095003-095003-12, 2010. https://doi.org/10.5006/1.3490308

[17] J.L.Crolet, N. Thevenot, and S. Nesic, "Role of conductive corrosion products in the protectiveness of corrosion layers", *Corrosion*, vol. 54, no. 3, pp. 194-203, 1998. https://doi.org/10.5006/1.3284844

[18] S. Nesic, J. Postlethwaite, and S. Olsen, "An electrochemical model for prediction of corrosion of mild steel in aqueous carbon dioxide solutions", *Corrosion*, vol. 52, no. 4, pp. 280-294, 1996. https://doi.org/10.5006/1.3293640

[19] Y. Zheng, B. Brown, and S. Nešić, "Electrochemical study and modeling of H2S corrosion of mild steel, *Corrosion*, vol. 70, no. 4, pp. 351-365, 2014. https://doi.org/10.5006/0937